The Distribution of Sulfur Dioxide and Other Infrared Absorbers on the Surface of Io

R. W. Carlson, W. D. Smythe, R. Lopes-Gautier, A.G. Davies, L. W. Kamp, J. A. Mosher

Jet Propulsion Laboratory, California Institute of Technology, Pasadena

L. A. Soderblom

United States Geological Survey, Flagstaff

F. E. Leader, R. Mehlman

Institute of Geophysics and Planetary Physics, University of California, Los Angeles

R. N. Clark

United States Geological Survey, Denver

F. P. Fanale

Planetary Geosciences Division, University of Hawaii, Honolulu

Submitted to
Geophysical Research Letters
April 4, 1997
Revised 11 August, 1997

Abstract

The Galileo Near Infrared Mapping Spectrometer was used to investigate the distribution and properties of sulfur dioxide over the surface of Io, and qualitative results for the anti-Jove hemisphere are presented here. S02, existing as a frost, is found almost everywhere, but with spatially variable concentration. The exceptions are volcanic hot spots, where high surface temperatures promote rapid vaporization and can produce SO_2-free areas. The pervasive frost, if fully covering the cold surface, has characteristic grain sizes of 30 to 100 μm, or greater. Regions of greater sulfur dioxide concentrations are found. The equatorial Colchis Regio area exhibits extensive snowfields with large particles (250 to 500 μm diameter, or greater) beneath smaller particles. A weak feature at 3.15 μm is observed and perhaps due to hydroxides, hydrates, or water. A broad absorption in the 1 μm region, which could be caused by iron-containing minerals, shows a concentration in Io's southern polar region, with an absence in the Pele plume deposition ring.

The distribution of condensed sulfur dioxide over the surface of Io is of interest because of its direct relationship to Io's active volcanoes, which vent gaseous SO_2 into the plumes, from which it subsequently deposits onto the cooler surface. The tenuous atmosphere (Lellouch et al., 1992; Ballester et al., 1994) can also play an important role, redistributing the material through sublimation, transport, and recondensation. The role of regional cold traps to sustain SO_2 snowfields (Fanale et al., 1982), Kerton et al., 1996) and their relation to local heat flow (McEwen, 1995), are important considerations, as well as the formation of ephemeral deposits migrating under solar influence (Hapke, 1989).

The surface distribution has been studied using ultraviolet and visible reflectance measurements (Nash et al., 1980; Nelson et al., 1980; McEwen, 1988, 1995; Sartoretti et al., 1994) and through infrared spectroscopy (e.g. Howell et al., 1984), but these studies provide conflicting descriptions of the SO_2 distribution. In the latter work, sulfur dioxide was inferred to be widely distributed and present in most terrains, in contrast to the preferential equatorial distribution suggested by direct imaging (McEwen, 1988, 1995). Ultraviolet measurements show significantly less S02 coverage (10-25%, Nash et al., 1980) than do infrared spectra (50-85°/0, Howell et al., 1984).

In this work we use measurements by the *Galileo* Near Infrared Mapping Spectrometer (NIMS, see Carlson et al. , 1992) to study the abundance of SO_2 over the anti-Jovian surface and investigate the distribution of other infrared absorbers. We use data from an observational sequence (termed G2INHRSPEC) obtained on 07 September 1995 during the second orbit around Jupiter. Among our many Io observations, we concentrate *on* these particular data because they were obtained at the highest NIMS spectral coverage (408 wavelength channels) and with relatively good spatial resolution (220 ktn per pixel), and because they include the interesting Pele - Pillan region and Colchis Regio, The subspacecraft point on Io during these measurements was near the equator and at 210° W, while the phase angle was 0.8-1.6°.

NIMS reflectance spectra of 10 show an abundance of features (see Fig. 1), most of which can be identified with condensed SO_2 using the molecular band assignments of Schmitt et al. (1994) and Nash and Betts (1995).

Other absorbers are evident in the spectra. A broad absorption in the 1.0 - 1.3 μm region, also shown in earlier spectra by Pollack et al. (1978), may be due to minerals containing iron, since ferrous materials show ubiquitous absorption in this region. The specific mineral(s) causing this feature in Io's spectrum is uncertain; Pollack et al. suggested iron-containing salts or feldspars. The distribution of this unknown absorber is discussed later.

The spectra show a weak but persistent absorption feature at 3.15 μm, and is probably the same feature previously reported by Salama et al. (1990) and Sand ford et al. (1994), who give positions of 3.12 μm and 3.16 μm respectively. It is tempting to ascribe the O-H stretch transition to this absorption, implying hydrated minerals, hydroxides, or even water. (H20 impurities in laboratory-grown SO_2 frosts show an absorption band centered at approximately 3.1 pm, c.f. Nash and Betts, 1995). If this feature is due to water, then it is a trace constituent whose concentration can be crudely estimated. Assuming that the oscillator strength for the ν_3 transition of water is approximately the same for the condensed and gaseous state, then for a measured equivalent width of -0.5 cm-1, a band strength of -200 cm-l per cm-atm (Pugh and Rae, 1976), and assuming that the average reflected photon suffers ten scattering events by millimeter-size SO_2 grains (see below), then an abundance of -4 ppm is found, Salama et al. (1990), suggesting that this feature is due to clusters of H_2O in sulfur dioxide ice,

estimated a water abundance of 1000 ppm. Laboratory work is needed to constrain the identification the 3.15 μm feature and derive abundances.

We now consider the spectrum and surface distribution of S02. The proper way to analyze the spectral data to determine abundances is to fit the entire spectrum with a radiative transfer model that includes areal (linear) and intimate mixing of other material, and allows for the vertical layering of grain sizes and impurity concentration. Such an analysis is beyond the scope of this report; here we provide merely a qualitative description of the sulfur dioxide distribution, using the depth of the strong 4.07 μm band and the equivalent widths for others to derive some interesting limits and show indications of vertical structure in the S02 snowfields.

We first note that the strong signature of sulfur dioxide, the intense 4.07 μm ($\nu_1 + \nu_3$) band, is present over all observed areas, except in regions of volcanic activity, where temperatures are high and sublimation rates are rapid. Even in these hot areas, with the limited spatial resolution of these data, few spectra are completely free of sulfur dioxide absorption. All observed wavelengths at the minima of the strong $\nu_1 + \nu_3$ band occur at 4.065 μm ± 0.013 μm, consistent with Laboratory frost spectra and inconsistent with adsorbed SO_2, for which the absorption minimum is shifted to ~ 4.04 μm (Nash and Betts, 1995). Thus, the dominant form of sulfur dioxide - at least for the hemisphere observed here - is frost, and this frost occurs widely over the surface. Both of these findings agree with Howell et al. (1984).

The absorption coefficient for the 4.07 μm band is quite large (Schmitt et al., 1994), so it is surprising that the center of this band in Io's spectrum never becomes completely dark. There are four possibilities for this behavior: 1) The band is saturated, but surface thermal emission produces the non-zero intensity. While this may be true for portions of the surface, we know from nightside measurements that it cannot be the major contributor. 2) There is areal or intimate mixing with other material which is bright at 4.07 **microns, for example sulfur and related** oxides (Hapke, 1989), 3) A surface layer of fine-grained sulfur dioxide, for which the small path lengths through the grains make absorption less important and can produce a moderately reflective scattering surface, even in the core of the band (Schmitt et al., 1994). 4) Existence of a thin, non-scattering glaze of SO_2 which *covers* a scattering surface.

While we cannot distinguish between the last three possibilities, we can place limits on the SO_2 surface grain sizes or glaze thickness. For the small particle scattering case (3), if we assume that the entire area of a pixel is covered by a frost that is optically thick in the core of the band, then the residual relative intensities at band minimum, (25 to 40°A in the equatorial region, 10 to 20°/0 at high latitudes) indicate grain sizes of - 30 μm at equatorial latitudes and - 100 μm in the polar regions. For a non-scattering but absorbing glaze, an average of Schmitt et al.'s absorption coefficients over the NIMS bandpass indicates glaze thicknesses of 10 to 20 pm. Of these two possibilities, the residual intensity, which is found to be relatively constant over the surface, is highly dependent *on* the thickness of the layer in the absorbing glaze case (4), whereas it is not for the scattering model, so the latter is preferred. In both cases, if the areal coverage is not complete, the grain sizes or glaze thickness would increase. Consequently the values quoted above are lower limits. However, the persistent occurrence of S02 throughout the areas sampled, and the extreme mobility of sulfur dioxide (Sandford and Allamandola, 1993) suggests near-complete coverage by a fine grained frost, which is sufficiently thin that underlying dark polar material can be seen in visible and ultraviolet wavelengths. Alternatively, this frost could be intimately mixed with the dark material (Howell et al,. 1984).

In addition to this possible pervasive frost coating, there can have localized concentrations of thicker deposits - snowfields - that become evident in other S02 absorption bands. We investigate qualitative properties of the sulfur dioxide distribution using maps of the equivalent widths for three bands, a weak band at 3.35 pm, a stronger one at 2.79 μm, and an even stronger on at 3.77 pm. We assume that these bands are formed solely by sulfur dioxide. The absorption depth of a feature, and the corresponding equivalent width, is a measure of the accumulated path length through the medium before the ray emerges from the medium. It depends on grain sizes of the refractive scatterers and number of scattering before escape, which in turn depends upon purity and optical depth of the medium. The dependencies are complex and nonlinear, so we use the equivalent widths as *qualitative* indicators of surface abundance. To reduce the influence of radiation-induced noise, a three-point running average was applied to all three dimensions of the spatial-spectral data cube, and for each pixel the equivalent widths were computed (see caption, Fig. 3 for wavelength intervals). Since we are performing averages over large areas, the resulting equivalent widths probably do not represent the maximum values. Results are shown in Fig. 2.

The 3.35 μm absorption strength of SO_2 is quite weak, and in order to obtain any significant absorption it is necessary to traverse long path lengths, accomplished in diffuse reflectance with large grains and many scattering. In fact, it is difficult to make sufficiently large grains in the laboratory to produce this feature (cf. the diffuse reflectance spectra of Nash and Betts (1995)). The strength of Io's 3.35 μm band is significant in the equatorial regions (Fig. 2D), indicating large grains. We can place lower limits to the grain sizes by assuming an optically thick, pure deposit of spherical grains of S02, and computing the predicted equivalent widths using radiative transfer theory and Schmitt et al.'s absorption coefficient. Fig. 3 shows the variation of equivalent width with particle size, indicating that grains of approximately 250 to 500 μm (or greater) are present in the equatorial regions of Io. If the S02 coverage is less than unity, or if other scatterers are present, the particle size estimate would be larger. This large-grained deposit shows good correlation with the *Voyager* bright areas and McEwen's (1988) SO_2 map.

The equatorial snowfield shows vertical structure. Theoretical equivalent widths for the stronger bands are also shown in Fig. 3, along with the equatorial measured values. While the weakest band indicates large grain sizes, the stronger bands, which are sensitive to much thinner and shallower depths in the medium, indicate smaller grains, being approximately 20 to 50 μm in diameter from the 3.77 μm band. Thus the snowfield is inhomogenous and the grain size increases with depth. This is reminiscent of terrestrial snow fields, where snow grains grow at the expense of smaller grains, reducing net surface tension energy. With continual deposition at the surface, the sizes increase with depth (and time). Subsurface growth and annealing of S02 crystals on Io has been discussed by Sandford and Allamondola (1993) and our results are consistent with their predictions.

For the rnidlatitude and polar regions, SO_2 is found to be present in variable concentrations, and shows correlation with the bright white regions in the *Voyager* map. These areas are probably not spatially resolved, so it is difficult to establish useful estimates or limits to abundance and sizes without performing detailed modelling.

The unknown absorber causing the 1-1.5 μm depression was mapped using the depth at 1.15 μm (relative to the 1.70 pm value) and shown in Fig. 2C. The most striking aspect is the concentration in the southern polar region, distinctly different than the sulfur dioxide maps. The material is absent in the plume deposition ring surrounding Pele but is present outside, suggesting that it is being covered by the plume ejects. It is

also depleted in the visibly dark regions north of Colchis Regio and the area around Heiseb Patera. Equatorial and mid-latitudes show less than half of the concentration evident in the southern polar region.

Acknowledgments. We thank Jan Yoshimizu for expert image processing and Elias Barbinis, Jim Shirley, and Paul Herrera for sequencing and playback assistance. The Galileo Project is funded by the NASA Solar System Exploration Division. The work described herein was performed at the Jet Propulsion Laboratory, California Institute of Technology, under contract with the National Aeronautics and Space Administration.

REFERENCES

Ballester, G. E., M. A. McGrath, D. F. Strobel, X. Zhu, P. D. Feldman, and H. W. Moos, Detection of the SO_2 atmosphere on Io with the Hubble Space Telescope, *Icarus* **111,** 2-17, 1994.

Carlson, R. W., P. R. Weissman, W. D. Smythe, J. C. Mahoney, and the NIMS Science and Engineering Teams, Near Infrared Mapping Spectrometer Experiment on Galileo, *Space Sci. Rev.* 60, 457-502, 1992.

Fanale, F. P., W. P. Banerdt, L. S. Elson, T. V. Johnson, and R. W. Zurek, Io's surface: Its phase composition and influence on Io's atmosphere and Jupiter's magnetosphere, in *Satellites of Jupiter,* edited by D. Morrison, pp. 756-781, Univ. of Arizona Press, Tucson, 1982.

Hapke, B., Bidirectional reflectance spectroscopy I. Theory, *J. Geophys. Res.* 86, 3039-3054, 1981.

Hapke, B., The surface of Io: A new model, *Icarus 79, 56-74, 1989.*

Howell, R. R., D. P. Cruickshank, and F. P. Fanale, Sulfur dioxide on Io: Spatial distribution and physical state, *Icarus* 57, 83-92, 1984.

Kerton, C. R., F. P. Fanale, and J. R. Salvail, The state of S02 on Io's surface, *J. Geophys. Res.* **101, 7555-7563,** 1996.

Lellouch, E., M. Belton, 1. De Pater, G. Paubert, S. Gulkis, and T. Encrenaz, The structure, stability, and global distribution of Io's atmosphere, *Icarus* **98,** 271-295, 1992.

McEwen, A. S., Global color and albedo variations on Io, *Icarus* **73,** 385-426, 1988

McEwen, A. S., SO_2-rich equatorial basins and epeirogony of Io, *Icarus* **113, 415-422,** 1995.

Nash, D. B., F. P. Fanale., and R. M. Nelson, SO_2 frost: UV-Visible reflectivity and Io surface coverage, *Geophys. Res. Lett.* **7, 64-67, 1980.**

Nash, D. B., and B. H. Betts, Laboratory infrared spectra (2.3-23 μm) of SO_2 phases: Applications to Io surface analysis, Icarus 117, 402-419, 1995.

Nelson, R. M., A. Lane, D. Matson, F. Fanale, D. Nash, and T. Johnson, Io's longitudinal distribution of sulfur dioxide frost, Science 210, 784-786, 1980.

Pollack, J. B., F. C. Witteborn, E. F. Erickson, D. W. Strecker, B. J. Baldwin, and T. E. Bunch, Near Infrared spectra of the Galilean satellites: Observations and compositional implications, *Icarus* **36, 271-303, 1978.**

Pugh, L. A., and K. N. Rae, Intensities from infrared spectra, in *Molecular Spectroscopy: Modem Research,* edited by K. N. Rae, Vol. 2, 165-227, 1976.

Salama, F., L. J. Allamandola, F. C. Witteborn, D. P. Cruikshank, S. A. Sand ford, and J. D. Bregman, The 2.5-5.0 μm spectra of Io: Evidence for H_2S and H_2O frozen in SO_2, *Icarus* **83, 66-82, 1990.**

Sandford, S. A., and L. J. Allamandola, The condensation and vaporization of ices containing SO_2, H2S, and CO_2: Implications for Io. *Icarus* **106, 478-488, 1993.**

Sandford, S. A., T. R. Gabelle, F. Salama, and D. Goorvitch, New narrow infrared absorption features in the spectrum of Io between 3600 and 3100 cm^{-1} (2.8-3.2 μm), *Icarus* **110, 292-302 (1994).**

Sartoretti, P., M. A. McGrath, and F. Paresce, Disk-resolved imaging of Io with the Hubble Space Telescope, *Icarus* **108, 272-284, 1994.**

Schmitt, B., C. deBergh, E. Lellouch, J.-P. Maillard, A. Barbe, and S. Doute, Identification of three absorption bands in the 2-pm spectrum of Io, *Icarus* **111,** *79-105, 1994.*

FIGURE CAPTIONS

Fig. 1, Spectrum of Io obtained by averaging data for the -200° meridian, avoiding obvious hot spots. SO_2 band identifications of Schmitt et al. (1994) and Nash and Betts (1995) are shown. The weak absorption at 3.15 μm may be due to the O-H stretch transition, i.e. a hydroxide, hydrate, or perhaps water. The broad absorption in the 1 μm region could be due to iron-containing minerals.

Fig. 2. Band Maps of Io. A) *Voyager* map corresponding to Galileo's view during the G2INHRSPEC observing sequence. The equatorial white area is Colchis Patera B) NIMS image at 5 μm, showing active volcanic hotspots. Pele and Pillan are at the left. C) Band depth map of the broad 1 μm absorber, where we plot the depth at 1.2 μm, relative to the value at 1.7 pm. The full depth of the band is larger (see Fig. 1). Note the enhancement in the southern polar region, D) Equivalent width map for the weak 3.35 μm band, showing equatorial concentration of SO_2. E) Equivalent width map for 2.79 pm band, and F) the 3.77 μm band.

Fig. 3. Curve-of-growth of equivalent widths and observed values for Colchis Regio. Theoretical values are computed for diffuse reflectance from an optically thick medium of pure SO_2 spheres, and are shown for the three bands considered as the thin lines. The range of observed equivalent widths for the Colchis region are indicated by the thicker portions. The inferred grain size varies with band strength, indicative of vertical variations in sizes of the SO_2 particles. The theoretical values were computed using Schmitt et al's. (1994) absorption cross sections and Hapke's (1981) radiative transfer formulation. The hi-hemispherical albedo was used for computing equivalent widths. The integration intervals used were: 3.28-3.43 pm, 2.71-2.87 μm, 3.69-3.82 pm.

Fig 1.

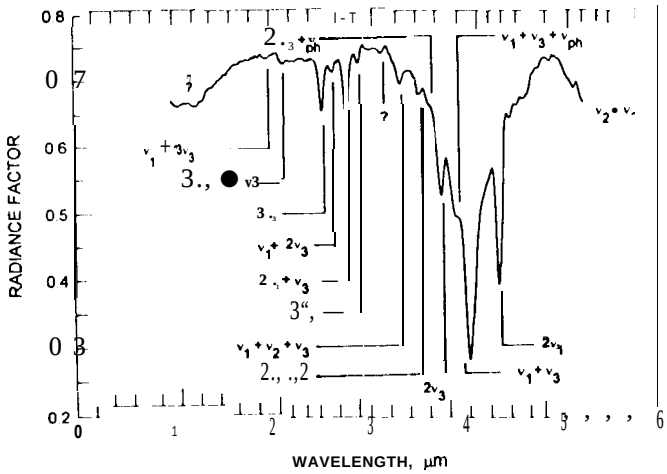
RADIANCE FACTOR
WAVELENGTH, μm

Fig. 3.

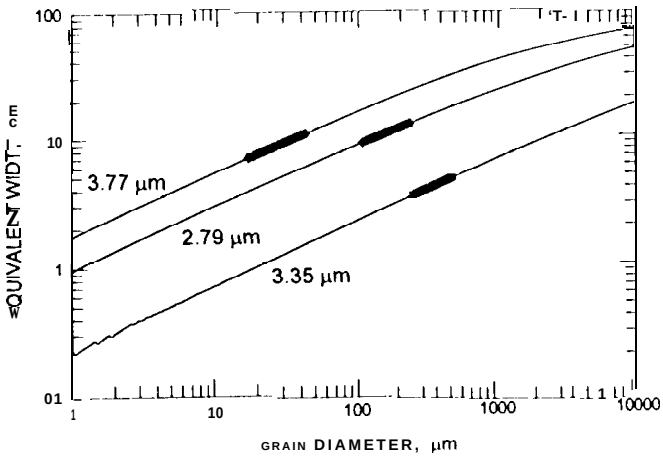
EQUIVALENT WIDTH, cm
3.77 μm
2.79 μm
3.35 μm
GRAIN DIAMETER, μm

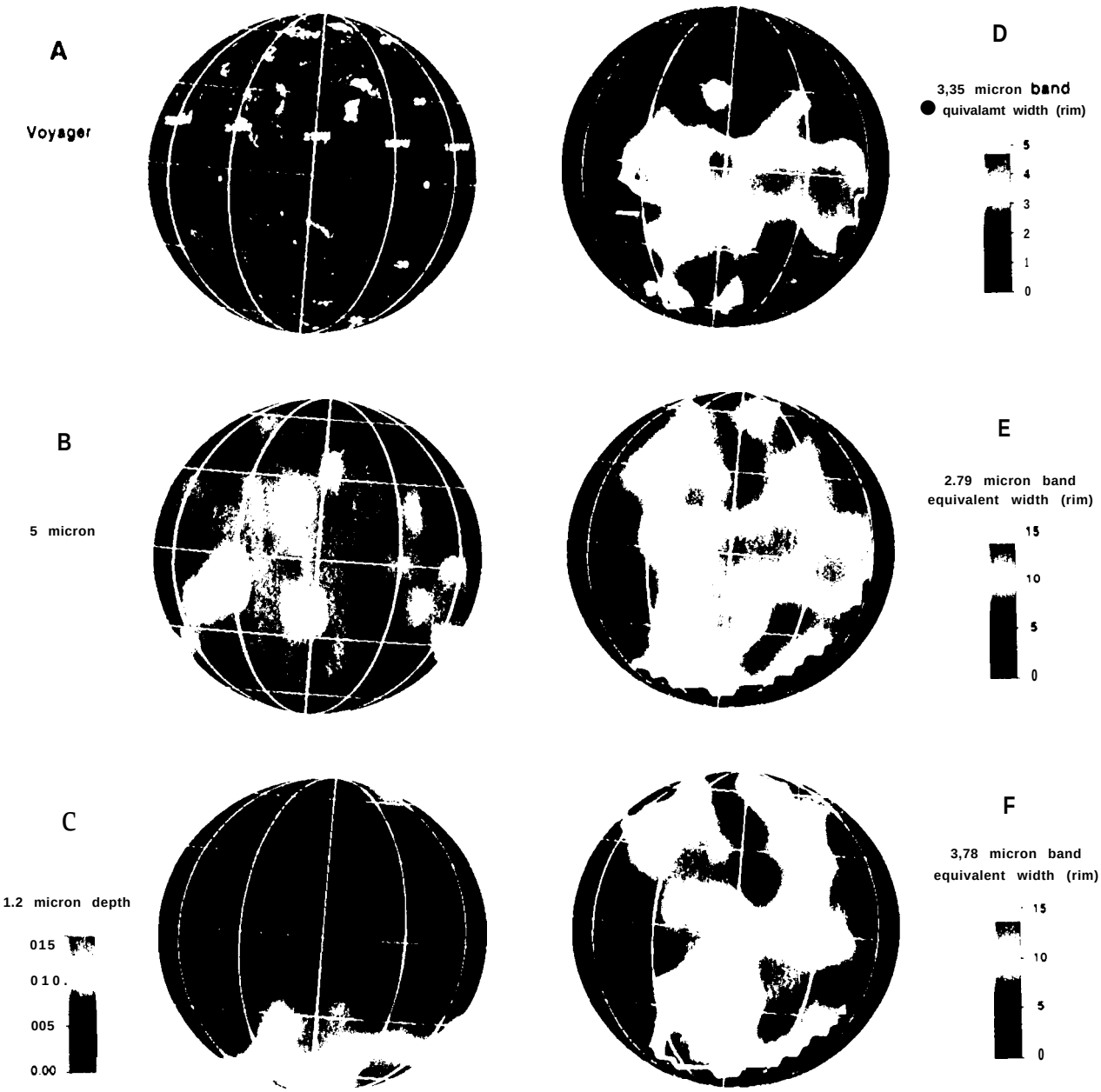
A
Voyager
B
5 micron
C
1.2 micron depth
015
010.
005
0.00
D
3,35 micron band
quivalamt width (rim)
5
4
3
2
1
0
E
2.79 micron band
equivalent width (rim)
15
10
5
0
F
3,78 micron band
equivalent width (rim)
15
10
5
0